THE JOURNAL OF BIOLOGICAL CHEMISTRY
Vol. 275, No. 41, Issue of October 13, pp. 31938–31945, 2000
Printed in U.S.A.

Anandamide Induces Apoptosis in Human Cells via Vanilloid Receptors

EVIDENCE FOR A PROTECTIVE ROLE OF CANNABINOID RECEPTORS*

Received for publication, June 29, 2000, and in revised form, July 20, 2000
Published, JBC Papers in Press, July 25, 2000, DOI 10.1074/jbc.M005722200

Mauro Maccarrone, Tatiana Lorenzon, Monica Bari, Gerry Melino, and Alessandro Finazzi-Agrò‡

From the Department of Experimental Medicine and Biochemical Sciences, University of Rome Tor Vergata, Via di Tor Vergata 135, I-00133 Rome, Italy

The endocannabinoid anandamide (AEA) is shown to induce apoptotic bodies formation and DNA fragmentation, hallmarks of programmed cell death, in human neuroblastoma CHP100 and lymphoma U937 cells. RNA and protein synthesis inhibitors like actinomycin D and cycloheximide reduced to one-fifth the number of apoptotic bodies induced by AEA, whereas the AEA transporter inhibitor AM404 or the AEA hydrolase inhibitor ATFMK significantly increased the number of dying cells. Furthermore, specific antagonists of cannabinoid or vanilloid receptors potentiated or inhibited cell death induced by AEA, respectively. Other endocannabinoids such as 2-arachidonoylglycerol, linoleoylethanolamide, oleoylethanolamide, and palmitoylethanolamide did not promote cell death under the same experimental conditions. The formation of apoptotic bodies induced by AEA was paralleled by increases in intracellular calcium (3-fold over the controls), mitochondrial uncoupling (6-fold), and cytochrome *c* release (3-fold). The intracellular calcium chelator EGTA-AM reduced the number of apoptotic bodies to 40% of the controls, and electrotransferred anti-cytochrome *c* monoclonal antibodies fully prevented apoptosis induced by AEA. Moreover, 5-lipoxygenase inhibitors 5,8,11,14-eicosatetraynoic acid and MK886, cyclooxygenase inhibitor indomethacin, caspase-3 and caspase-9 inhibitors Z-DEVD-FMK and Z-LEHD-FMK, but not nitric oxide synthase inhibitor *N*ω-nitro-L-arginine methyl ester, significantly reduced the cell death-inducing effect of AEA. The data presented indicate a protective role of cannabinoid receptors against apoptosis induced by AEA via vanilloid receptors.

Anandamide (arachidonoylethanolamide, AEA)[1] belongs to an emerging class of endogenous lipids including amides and esters of long chain polyunsaturated fatty acids and collectively indicated as "endocannabinoids" (1). In fact, AEA has been isolated and characterized as an endogenous ligand for cannabinoid receptors in the central nervous system (CB1 subtype) and peripheral immune cells (CB2 subtype). AEA is released from depolarized neurons, endothelial cells and macrophages (2), and mimics the pharmacological effects of Δ^9-tetrahydrocannabinol, the active principle of hashish and marijuana (3). Recently, attention has been focused on the possible role of AEA and other endocannabinoids in regulating cell growth and differentiation, which might account for some pathophysiological effects of these lipids. An anti-proliferative action of AEA has been reported in human breast carcinoma cells, due to a CB1-like receptor-mediated inhibition of the action of endogenous prolactin at its receptor (4). An activation of cell proliferation by AEA has been reported instead in hematopoietic cell lines (5). Moreover, preliminary evidence that the immunosuppressive effects of AEA might be associated with inhibition of lymphocyte proliferation and induction of programmed cell death (PCD or apoptosis) has been reported (6), and growing evidence is being collected that suggests that AEA might have pro-apoptotic activity, both *in vitro* (7) and *in vivo* (8). This would extend to endocannabinoids previous observations on Δ^9-tetrahydrocannabinol, shown to induce PCD in glioma tumors (8), glioma cells (9), primary neurons (10), hippocampal slices (10), and prostate cells (11). However, the mechanism of AEA-induced PCD is unknown. The various effects of AEA in the central nervous system and in immune system (reviewed in Refs. 1–3), as well as its ability to reduce the emerging pain signals at sites of tissue injury (12), are terminated by a rapid and selective carrier-mediated uptake of AEA into cells (13), followed by its degradation to ethanolamine and arachidonic acid by the enzyme fatty acid amide hydrolase (FAAH) (14). Recently, we showed that human neuroblastoma CHP100 cells and human lymphoma U937 cells do have these tools to eliminate AEA (15). Therefore, these cell lines were chosen to investigate how AEA and related endocannabinoids induce apoptosis and how the removal and degradation of AEA are related to this process. The existence of a neuroimmune axis appears to be confirmed by the finding that endocannabinoids elicit common responses in these two cell types.

EXPERIMENTAL PROCEDURES

Materials—Chemicals were of the purest analytical grade. Anandamide (arachidonoylethanolamide, AEA), actinomycin D, cycloheximide, 5,8,11,14-eicosatetraynoic acid (ETYA), indomethacin, cytochrome *c*, cyclosporin A,

* This work was supported in part by Istituto Superiore di Sanità (III AIDS Program), by Ministero dell'Università e della Ricerca Scientifica e Tecnologica, Rome (to A.F.A.), and by Telethon Grant E872 (to G. M.). The costs of publication of this article were defrayed in part by the payment of page charges. This article must therefore be hereby marked "*advertisement*" in accordance with 18 U.S.C. Section 1734 solely to indicate this fact.

‡ To whom correspondence should be addressed. Tel./Fax: 39-06-72596468; E-mail: Finazzi@uniroma2.it.

[1] The abbreviations used are: AEA, anandamide (arachidonoylethanolamide); 2-AG, 2-arachidonoylglycerol; AM404, *N*-(4-hydroxyphenyl)-arachidonoylamide; ATFMK, arachidonoyl-trifluoromethyl ketone; Caps, capsazepine; CBD, cannabidiol; CB1/2R, type 1/2 cannabinoid receptor; AM, acetoxymethyl ester; ELISA, enzyme-linked immunosorbent assay; ETYA, 5,8,11,14-eicosatetraynoic acid; FAAH, fatty acid amide hydrolase; LEA, linoleoylethanolamide; L-NAME, *N*ω-nitro-L-arginine methyl ester; OEA, oleoylethanolamide; PBS, phosphate-buffered saline; PEA, palmitoylethanolamide; VR, vanilloid receptor; Z-DEVD-FMK, Z-Asp(OCH_3)-Glu(OCH_3)-Val-Asp(OCH_3)-fluoromethyl ketone; Z-LEHD-FMK, Z-Leu-Glu(OCH_3)-His-Asp (OCH_3)-fluoromethyl ketone; GAM-AP, goat anti-mouse alkaline phosphatase; PCD, programmed cell death.

and *N*ω-nitro-L-arginine methyl ester (L-NAME) were purchased from Sigma. 2-Arachidonoylglycerol (2-AG), arachidonoyltrifluoromethyl ketone (ATFMK) and *N*-(4-hydroxyphenyl)arachidonoylamide (AM404) were from Research Biochemicals International. EGTA-AM, capsaicin ([*N*-(4-hydroxy-3-methoxy-phenyl)methyl]-8-methyl-6-nonenamide), capsazepine (*N*-[2-(4-chlorophenyl)ethyl]-1,3,4,5-tetrahydro-7,8-dihydroxy-2H-2-benzazepine-2-carbothioamide, Caps), caspase-3 inhibitor II (Z-Asp(OCH_3)-Glu(OCH_3)-Val-Asp(OCH_3)-fluoromethyl ketone, Z-DEVD-FMK), and caspase-9 inhibitor I (Z-Leu-Glu(OCH_3)-His-Asp(OCH_3)-fluoromethyl ketone, Z-LEHD-FMK) were from Calbiochem. [^{3}H]AEA (223 Ci/mmol) and [^{3}H]CP55,940 (126 Ci/mmol) were purchased from NEN Life Science Products. *N*-Piperidino-5-(4-chlorophenyl)-1-(2,4-dichlorophenyl)-4-methyl-3-pyrazolecarboxamide (SR141716) and *N*-[1(*S*)-endo-1, 3, 3-trimethylbicyclo[2.2.1]heptan-2-yl]-5-(4-chloro-3-methylphenyl)-1-(4-methylbenzyl)-pyrazole-3-carboxamide (SR144528) were a kind gift from Sanofi Recherche (Montpellier, France). Palmitoylethanolamide (PEA), oleoylethanolamide (OEA), and linoleoylethanolamide (LEA) were synthesized and characterized (purity >96% by gas-liquid chromatography) as reported (15). Cannabidiol (CBD) was a kind gift from Dr. M. Van der Stelt (Utrecht University, The Netherlands). 5,5′,6,6′-Tetrachloro-1,1′,3,3′-tetraethylbenzimidazol-carbocyanine iodide (JC-1) and 1-[2-amino-5-(2,7-dichloro-6-hydroxy-3-oxy-9-xanthenyl)-phenoxy]-2-[2-amino-5-methyl-phenoxy]ethane-*N,N,N′,N′*-tetraacetoxymethyl ester (Fluo-3 AM) were from Molecular Probes. Anti-cytochrome *c* monoclonal antibodies (clone 7H8.2C12 and clone 6H2.B4) were purchased from PharMingen, and goat anti-mouse alkaline phosphatase conjugates (GAM-AP) were from Bio-Rad. Non-immune mouse serum was from Nordic Immunology (Tilburg, The Netherlands).

Cell Culture and Treatment—Human neuroblastoma CHP100 cells were cultured as reported (15), in a 1:1 mixture of Eagle's minimal essential medium plus Earle's salts and Ham's F-12 media (Flow Laboratories Ltd., Ayrshire, Scotland, UK), supplemented with 15% heat-inactivated fetal bovine serum, sodium bicarbonate (1.2 g/l), 15 mM Hepes buffer, 2 mM L-glutamine, and 1% non-essential amino acids. Human lymphoma U937 and leukemia DAUDI cells were cultured in RPMI 1640 medium (Life Technologies, Inc.) supplemented with 25 mM Hepes, 2.5 mM sodium pyruvate, 100 units/ml penicillin, 100 μg/ml streptomycin, and 10% heat-inactivated fetal calf serum (15). Rat C6 glioma cells, a kind gift from Dr. Dale G. Deutsch (Department of Biochemistry and Cell Biology, State University of New York, Stony Brook), were cultured in Ham's F-12 medium supplemented with 10% fetal calf serum as described (9). Cells were maintained at 37 °C in a humidified atmosphere with 5% CO_2 and were fed every 3–4 days. Before each treatment, cells were washed twice with sterile, Ca^{2+} and Mg^{2+}-free phosphate-buffered saline (PBS), and then they were resuspended in sterile PBS at a concentration of 10^6 cells/ml. Cell suspensions were incubated for 30 min at 37 °C in the presence of various concentrations (up to 10 μM) of endocannabinoids dissolved in methanol, and they were then resuspended in their culture media for the indicated periods. Control cells were incubated with the same volumes of vehicle alone (up to 10 μl/ml PBS). The interference of various compounds with the effects of AEA was assessed by incubating together CHP100 or U937 cells with each substance and AEA.

Electrotransfer of anti-cytochrome *c* monoclonal antibodies (clone 6H2.B4, which recognizes the native form of cytochrome *c*; 200 μg/test) into U937 cells (10^6 cells/test) was performed with a Gene Pulser II Plus apparatus (Bio-Rad). Exponentially decaying pulses were generated and delivered to cells suspended in PBS (0.7 ml/test) in sterile disposable electroporation cuvettes (Bio-Rad) of 0.4-cm path length (16). U937 cells were electroporated at a capacitance of 125 microfarads and a field strength of 800 V/cm, with a time constant (τ) of 1.5 ± 0.2 ms. Control cells were electroporated under the same experimental conditions, in the presence of non-immune mouse serum (200 μg/test). After electroporation, cells were kept for 5 min at 4 °C, and they were then washed twice in PBS and treated with AEA as described for the non-electroporated cells. Under these experimental conditions, approximately 1.0 pg/cell (2.5 μg/mg protein) of monoclonal antibodies was incorporated (16).

Evaluation of Cell Death—After incubation for the indicated periods in culture medium, floating and enzymatically detached cells were collected together by centrifugation at 200 × *g* for 5 min. Viability was estimated by trypan blue dye exclusion in a Neubauer hemocytometer. Apoptosis was estimated in all experiments by cytofluorimetric analysis in a FACScalibur flow cytometer (Becton Dickinson), which quantified apoptotic body formation in dead cells by staining with propidium iodide (50 μg/ml, pretreated also with RNase to reduce noise), as reported (17). Cells were fixed using a methanol:acetone (4:1 v/v) solution, 1:1 in PBS, at −20 °C, and were stored at 4 °C. Cells were excited at 488 nm using a 15-milliwatt argon laser, and the fluorescence was monitored at 570 nm. Events were triggered by the FSC signal and gated for FL2-A/FL2-W to skip aggregates. Ten thousand events were evaluated using the Cell Quest Program. Controls of different cell lines contained less than 4.0 ± 1.0 apoptotic bodies every 100 cells analyzed. PCD was evaluated also by the cell-death detection ELISA kit (Roche Molecular Biochemicals), based on the evaluation of DNA fragmentation by an immunoassay for histone-associated DNA fragments in the cell cytoplasm (18).

Determination of Anandamide Uptake and Fatty Acid Amide Hydrolase (FAAH)—The uptake of [^{3}H]AEA by intact C6 or DAUDI cells was studied as described (15). Cells were washed in PBS and resuspended in the respective serum-free culture media, at a density of 2×10^6 cells/ml. Cell suspensions (1 ml/test) were incubated for different time intervals, at 37 °C, with 200 nM [^{3}H]AEA; then they were washed three times in 2 ml of culture medium containing 1% bovine serum albumin and were finally resuspended in 200 μl of PBS. Membrane lipids were then extracted (18), resuspended in 0.5 ml of methanol, and mixed with 3.5 ml of Sigma-Fluor liquid scintillation mixture for non-aqueous samples (Sigma), and radioactivity was measured in a LKB1214 Rackbeta scintillation counter (Amersham Pharmacia Biotech). To discriminate non-carrier-mediated from carrier-mediated transport of AEA into cell membranes, control experiments were made at 4 °C (15). Incubations (15 min) were also carried out with different concentrations of [^{3}H]AEA, in the range 0–1000 nM, in order to determine apparent K_m and V_{max} of the uptake by Lineweaver-Burk analysis (in this case, the uptake at 4 °C was subtracted from that at 37 °C). AEA uptake was expressed as picomoles of AEA taken up per min per mg of protein.

Fatty acid amide hydrolase (EC 3.5.1.4; FAAH) activity was assayed in C6 or DAUDI cell extracts by measuring the release of [^{3}H]arachidonic acid from [^{3}H]AEA, using reversed phase high performance liquid chromatography as reported (15). FAAH activity was expressed as picomoles of arachidonate released per min per mg of protein. Kinetic studies were performed using different concentrations of [^{3}H]AEA (in the range 0–25 μM), and the kinetic constants (K_m, V_{max}) were calculated by fitting the experimental points in a Lineweaver-Burk plot with a linear regression program (Kaleidagraph 3.0.4). Straight lines with *r* values >0.95 were obtained.

Cannabinoid Receptor Binding Assay—CHP100, U973, C6, or DAUDI cells (2×10^8) were pelleted and resuspended in 8 ml of buffer A (2 mM Tris-EDTA, 320 mM sucrose, 5 mM $MgCl_2$, pH 7.4) and then were homogenized in a Potter homogenizer and centrifuged at 1000 × *g* for 10 min (19). The supernatant was recovered and combined with the supernatants obtained from two subsequent centrifugations at 1000 × *g* of the pellet. Combined supernatant fractions were centrifuged at 40000 × *g* for 30 min, and the resulting pellet was resuspended in assay buffer B (50 mM Tris-HCl, 2 mM Tris-EDTA, 3 mM $MgCl_2$, pH 7.4), to a protein concentration of 1 mg/ml (19). The membrane preparation was divided in aliquots, quickly frozen in liquid nitrogen, and stored at −80 °C for no longer than 1 week. These membrane fractions, as well as those prepared from the brain of Wistar rats (male, weighting 250–280 g), were used in rapid filtration assays with the synthetic cannabinoid [^{3}H]CP55,940, as described previously (19). Data of displacement of 400 pM [^{3}H]CP 55,940 by various concentrations of AEA (in the range 10^{-12} to 10^{-6} M) were elaborated by the GraphPad program (GraphPad Software for Science), calculating the inhibition constant (K_i) as reported (20). Unspecific binding was determined in the presence of 10 μM AEA (19, 20). Binding of [^{3}H]AEA to cells was assessed using the same membrane preparations and the same filtration assays as those described above for the cannabinoid receptors binding.

Measurement of Mitochondrial Uncoupling and Intracellular Calcium—Mitochondrial uncoupling and intracellular calcium concentration were evaluated by flow cytometric analysis in a FACScalibur Flow Cytometer (Becton Dickinson).

Mitochondrial uncoupling was measured using the fluorescent probe JC-1, as described (21). JC-1 (dissolved in dimethyl sulfoxide) was used at 20 μM final concentration. Control cells were treated with vehicle alone (1% of the final volume). After the treatment, CHP100 or U937 cells were washed in PBS and incubated 20 min at 37 °C. Cells were then analyzed in a FL1/FL2 dot plot (530 nm/570 nm), gating on morphologically normal cells.

Cytoplasmic free calcium was measured using the fluorescent Ca^{2+} indicator Fluo-3 AM, as reported (22). CHP100 or U937 cells were collected by centrifugation and washed twice in Ca^{2+}- and Mg^{2+}-free PBS. Then, Fluo-3 AM (10 μM dissolved in dimethyl sulfoxide) was added, and cells were incubated 40 min at 37 °C in the dark and frequently shaken manually. Control cells were treated with vehicle

alone (1% of the final volume). Cells were then collected by centrifugation and resuspended in culture medium without fetal bovine serum. Fluo-3 AM fluorescence was recorded on a linear scale at 530 nm (bandwidth 30 nm), at a flow rate of approximately 1000 cells/s. Mean fluorescence values for 3000 events were registered every 10 s. Changes in mean fluorescence were plotted *versus* time.

Immunochemical Analysis—SDS-polyacrylamide gel electrophoresis (12%) under reducing conditions and electroblotting onto 0.45-μm nitrocellulose filters (Bio-Rad) were performed on cell extracts (25 μg/lane), prepared as reported (23). Prestained molecular mass markers (Bio-Rad) were carbonic anhydrase (37 kDa), soybean trypsin inhibitor (27 kDa), and lysozyme (19 kDa). Immunodetection of cytochrome *c* on nitrocellulose filters was performed with specific anti-cytochrome *c* monoclonal antibodies (clone 7H8.2C12, which recognizes the denatured form of cytochrome *c*), diluted 1:250. Goat anti-mouse immunoglobulins conjugated with alkaline phosphatase (GAM-AP) were used as secondary antibody at 1:2000 dilution. The amount of cytochrome *c* released into the cytosol of CHP100 or U937 cells 8 h after treatment (23) was quantified by enzyme-linked immunosorbent assay (ELISA). Cell extracts (25 μg/well) were prepared as reported (23) and were reacted with anti-cytochrome *c* monoclonal antibodies (clone 7H8.2C12), diluted 1:250. GAM-AP were used as secondary antibody at 1:2000 dilution. Color development of the alkaline phosphatase reaction was recorded at 405 nm, using *p*-nitrophenyl phosphate as substrate (15). The absorbance values of the unknown samples were within the linearity range of the ELISA test, assessed by calibration curves with known amounts of cytochrome *c* (in the range 0–500 ng/well).

Statistical Analysis—Data reported in this paper are the mean (±S.D.) of at least three independent determinations, each in duplicate. Statistical analysis was performed by the Student's *t* test, elaborating experimental data by means of the InStat program (GraphPad Software for Science).

RESULTS

AEA-induced PCD Is Not Mediated by CB1 or CB2 Receptors and Is Potentiated by Inhibitors of AEA Degradation—Treatment of human neuroblastoma CHP100 cells and human lymphoma U937 cells with AEA led to apoptotic body formation in a dose- (Fig. 1*A*) and time- (Fig. 1*B*) dependent manner. Detection by ELISA of DNA fragments in the cell cytosols under the same experimental conditions confirmed the cytofluorimetric data (Fig. 1*C*). Apoptosis at 48 h was significant in both cell lines already at 0.25 μM AEA (approximately 2.5-fold over the control) and reached a level of 6.0-fold over the control at 1 μM AEA (Fig. 1*A*). These concentrations are in the physiological range (24). Time course experiments showed that 1 μM AEA induced a significant increase in apoptotic bodies 24 h after treatment (2.5-fold over the control) and a maximum of 6-fold the control after 48 h (Fig. 1*B*). Unlike AEA, 2-AG and other endocannabinoids failed to induce significant cell death in CHP100 or U937 cells (Table I).

In order to investigate the possible role of cannabinoid receptors on PCD induced in CHP100 or U937 cells by AEA, two specific CBR antagonists were used as follows: SR141716 and SR144528, which bind CB1R and CB2R, respectively (3). Neither SR141716 nor SR144528, even if used at an excess concentration of 5 μM, could significantly prevent the AEA-induced toxicity, suggesting that the effect was not mediated by "classical" CB1 or CB2 receptors (Table II). In line with these data, the synthetic cannabinoid [^{3}H]CP55.940, a high affinity ligand for both CB1 and CB2 receptors (3), did not bind to human neuroblastoma or lymphoma cells, suggesting that they had no functional cannabinoid receptors on their surface (Fig. 2). Instead rat brain, used as a positive control, did bind [^{3}H]CP55.940, which was displaced by AEA (Fig. 2, *inset*) with an inhibition constant (K_i = 30 ± 4 nM) close to that previously reported (20). Either the inhibitor of AEA transporter AM404 (25) or the FAAH inhibitor ATFMK (26), each used at 10 μM, significantly increased (up to approximately 180 or 165% of the control, respectively) the AEA toxicity (Table II). On the other hand, actinomycin D and cycloheximide (both at 10 μg/ml) reduced AEA-induced PCD in CHP100 cells down to approximately 20 or 30% of the control, respectively (Table II). Superimposable results were observed with the human lymphoma U937 cell line (Table II).

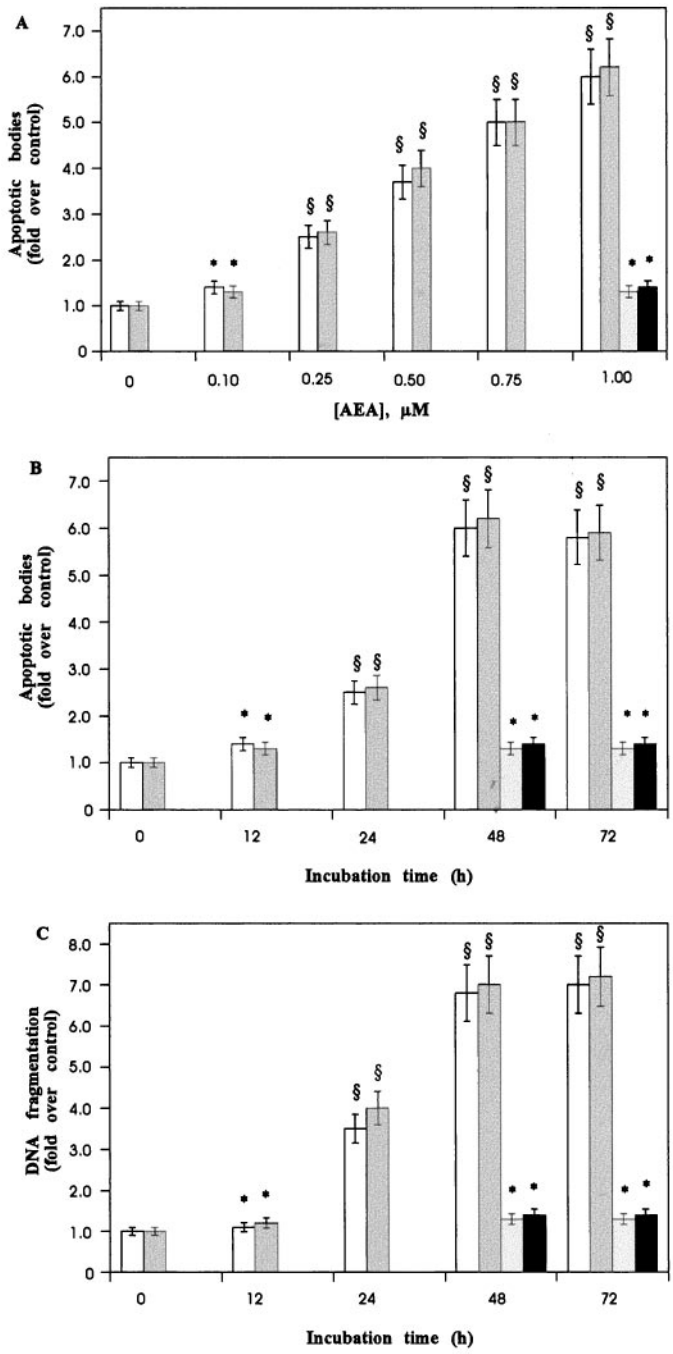

FIG. 1. **Induction of apoptosis by AEA in different cell lines.** AEA induced apoptotic body formation and DNA fragmentation in human neuroblastoma CHP100 cells (*white bars*) and human lymphoma U937 cells (*gray bars*). *A*, the number of apoptotic bodies was measured at 48 h, and *B*, it was measured in cells treated with 1 μM AEA. *C*, DNA fragmentation was measured in the same samples as in *B*. Rat glioma C6 cells (*light gray bars*) and human leukemia DAUDI cells (*black bars*) did not show apoptotic body formation or DNA fragmentation under the same experimental conditions. *, $p > 0.05$ compared with control; §, $p < 0.01$ compared with control.

AEA-induced PCD Is Mediated by Vanilloid Receptors—CHP100 and U937 cells were able to bind [^{3}H]AEA, according to a saturable process with an apparent affinity constant of 75 ± 10 nM (Fig. 3*A*). Cold AEA, but not 2-AG, SR141716 or SR144528 (each used at 1 μM), displaced 200 nM [^{3}H]AEA from

TABLE I

Effect of AEA analogues on apoptotic body formation, mitochondrial uncoupling and intracellular calcium concentration in CHP100 cells

Values refer to measurements performed 48 h (apoptotic bodies), 6 h (mitochondrial uncoupling), or 6 min (intracellular calcium) after the addition of each compound. In all analyses, U937 cells showed results superimposable to those obtained with CHP100 cells, omitted for the sake of clarity.

Compound (1 μM)	Apoptotic bodies	Mitochondrial uncoupling	Intracellular calcium
	-fold over control	*-fold over control*	*-fold over control*
None	1.0	1.0	1.0
2-AG	1.4 ± 0.2[a]	1.4 ± 0.2[a]	1.4 ± 0.2[a]
LEA	1.4 ± 0.2[a]	1.4 ± 0.2[a]	1.3 ± 0.2[a]
OEA	1.3 ± 0.2[a]	1.3 ± 0.2[a]	1.2 ± 0.2[a]
PEA	1.4 ± 0.2[a]	1.2 ± 0.2[a]	1.3 ± 0.2[a]

[a] $p > 0.05$ compared with control.

TABLE II

Effect of various compounds on AEA-induced cell death in human CHP100 and U937 cells

Values were expressed as percentage of the number of apoptotic bodies induced by 1 μM AEA after 48 h (see Fig. 1A). Treatment of either cell line with any of the compounds listed, in the absence of AEA, did not significantly affect cell death under the same experimental conditions.

Compound	Apoptotic bodies	
	CHP100	U937
	%	
None	100	100
SR141716 (5 μM)	85 ± 9[a]	85 ± 9[a]
SR144528 (5 μM)	90 ± 9[a]	90 ± 9[a]
AM404 (10 μM)	180 ± 18[b]	175 ± 18[b]
ATFMK (10 μM)	165 ± 17[b]	170 ± 17[b]
Actinomycin D (10 μg/ml)	20 ± 2[b]	25 ± 3[b]
Cycloheximide (10 μg/ml)	30 ± 3[b]	30 ± 3[b]
EGTA-AM (50 μM)	40 ± 4[b]	35 ± 4[b]
Cyclosporin A (10 μM)	85 ± 9[a]	85 ± 9[a]
ETYA (10 μM)	50 ± 5[b]	40 ± 4[b]
MK886 (10 μM)	55 ± 6[b]	45 ± 5[b]
Indomethacin (10 μM)	35 ± 4[b]	30 ± 3[b]
L-NAME (50 μM)	90 ± 9[a]	90 ± 9[a]
CBD (10 μM)	85 ± 9[a]	90 ± 9[a]
Caps (10 μM)	30 ± 3[b]	30 ± 3[b]
Z-DEVD-FMK (50 μM)	25 ± 3[b]	20 ± 2[b]
Z-LEHD-FMK (50 μM)	30 ± 3[b]	25 ± 3[b]

[a] $p > 0.05$ compared with AEA-treated samples.
[b] $p < 0.01$ compared with AEA-treated samples.

the binding site (Fig. 3*B*). Also, 1 μM cannabidiol (CBD), a selective antagonist of a newly discovered type of cannabinoid receptor (27), failed to affect the binding of 200 nM [^{3}H]AEA to CHP100 or U937 cells, whereas 1 μM capsazepine (Caps), a selective antagonist of vanilloid receptors (28), fully displaced it (Fig. 3*B*). Interestingly, 10 μM CBD did not protect CHP100 or U937 cells against PCD induced by 1 μM AEA, whereas 10 μM Caps led to a 30% reduction of apoptotic bodies in both cell lines (Table II). Moreover, when we treated CHP100 or U937 cells with 1 μM capsaicin, the physiological agonist of vanilloid receptors (28), we found a 5-fold increase in apoptotic bodies after 48 h, which resembled the effect of 1 μM AEA on these cells (Fig. 1*A*).

Cannabinoid Receptors Prevent AEA-induced PCD—Rat glioma C6 cells and human leukemia DAUDI cells were found to have a specific AEA transporter, with apparent K_m and V_{max} values for AEA of 0.15 ± 0.02 μM and 40 ± 4 pmol·min^{-1}·mg protein^{-1} (C6 cells) and 0.10 ± 0.01 μM and 150 ± 15 pmol·min^{-1}·mg protein^{-1} (DAUDI cells). FAAH activity, which has been already reported in C6 cells (29), was found to depend on AEA concentration according to a Michaelis-Menten kinetics in these cells and in DAUDI cells (not shown), with apparent K_m of 5.0 ± 0.5 μM and V_{max} of 135 ± 15 pmol·min^{-1}·mg protein^{-1} (C6), and 5.0 ± 0.5 μM and 450 ± 50 pmol·min^{-1}·mg protein^{-1} (DAUDI). These kinetic parameters of AEA transporter and FAAH in C6 and DAUDI cells closely resembled those measured in CHP100 or U937 cells, respectively (15). Moreover, C6 cells have been reported to express CB1R on their surface (9), whereas in DAUDI cells the mRNA for the CB2 receptor subtype has been found (30). Consistently, these cells were able to bind [^{3}H]CP55.940, which was displaced by 0.1 μM SR141716 in C6 cells or 0.1 μM SR144528 in DAUDI cells and by 1 μM AEA in both cell types (Fig. 2). Quite interestingly, neither cell line showed apoptotic body formation or DNA fragmentation when treated with 1 μM AEA under the experimental conditions previously tested with CHP100 or U937 cells (Fig. 1). However, at 10 μM AEA concentration a 3.5–4.0-fold increase in PCD after 48 h (Table III) was observed, an effect that was enhanced in C6 cells by 1 μM SR141716, but not by SR144528, whereas in DAUDI cells the opposite was found (Table III). Inhibition of the AEA transporter by 10 μM AM404 almost doubled apoptotic body formation induced by AEA in both cell lines, and this effect was additive to that of SR141716 in C6 cells and of SR144528 in DAUDI cells (Table III). Apoptosis induced by 10 μM AEA in C6 or DAUDI cells was reduced to approximately 40% by 10 μM Caps, whereas CBD at the same concentration was ineffective (Table III). Remarkably, C6 and DAUDI cells were able to bind [^{3}H]AEA (400 ± 40 or 350 ± 40 cpm respectively, upon incubation with 200 nM [^{3}H]AEA), which was fully displaced by 1 μM SR141716 + 1 μM Caps (C6 cells) or 1 μM SR144528 + 1 μM Caps (DAUDI cells). Caps alone displaced approximately 30% [^{3}H]AEA from each cell type, under the same experimental conditions.

AEA Induces Mitochondrial Uncoupling, Intracellular Calcium Rise, and Cytochrome c Release—AEA led to a dose-de-

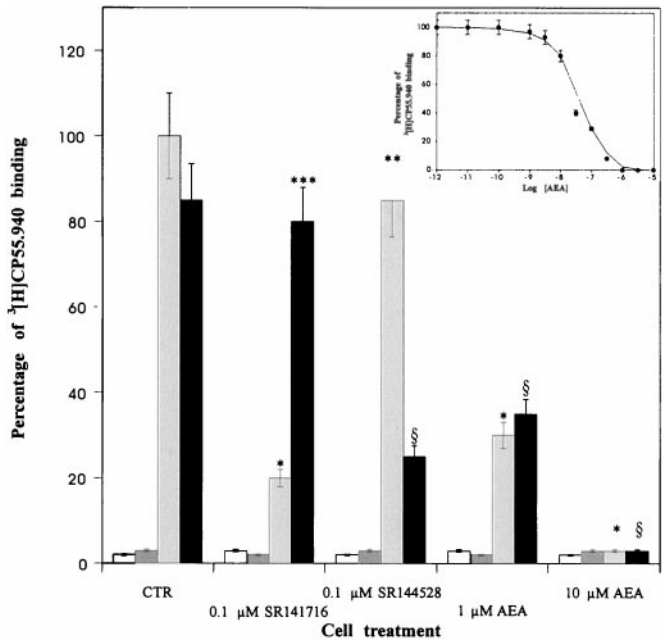

FIG. 2. **Analysis of functional cannabinoid receptors in different cell lines.** Binding of the synthetic cannabinoid [^{3}H]CP55.940 (400 pM) to CHP100 (*white bars*), U937 (*gray bars*), C6 (*light gray bars*), and DAUDI (*black bars*) cells and displacement by 0.1 μM SR141716, 0.1 μM SR144528, or 1 μM AEA. Unspecific binding was measured in the presence of 10 μM AEA. Values were expressed as percentage of the maximum (100% = 1000 ± 100 cpm). *Inset,* binding of [^{3}H]CP55.940 (400 pM) by rat brain membranes and displacement by various concentrations of AEA. Values were expressed as percentage of the maximum (100% = 1000 ± 100 cpm). *CTR*, control. *, $p < 0.01$ compared with control C6 cells; **, $p > 0.05$ compared with control C6 cells; ***, $p > 0.05$ compared with control DAUDI cells; §, $p < 0.01$ compared with control DAUDI cells.

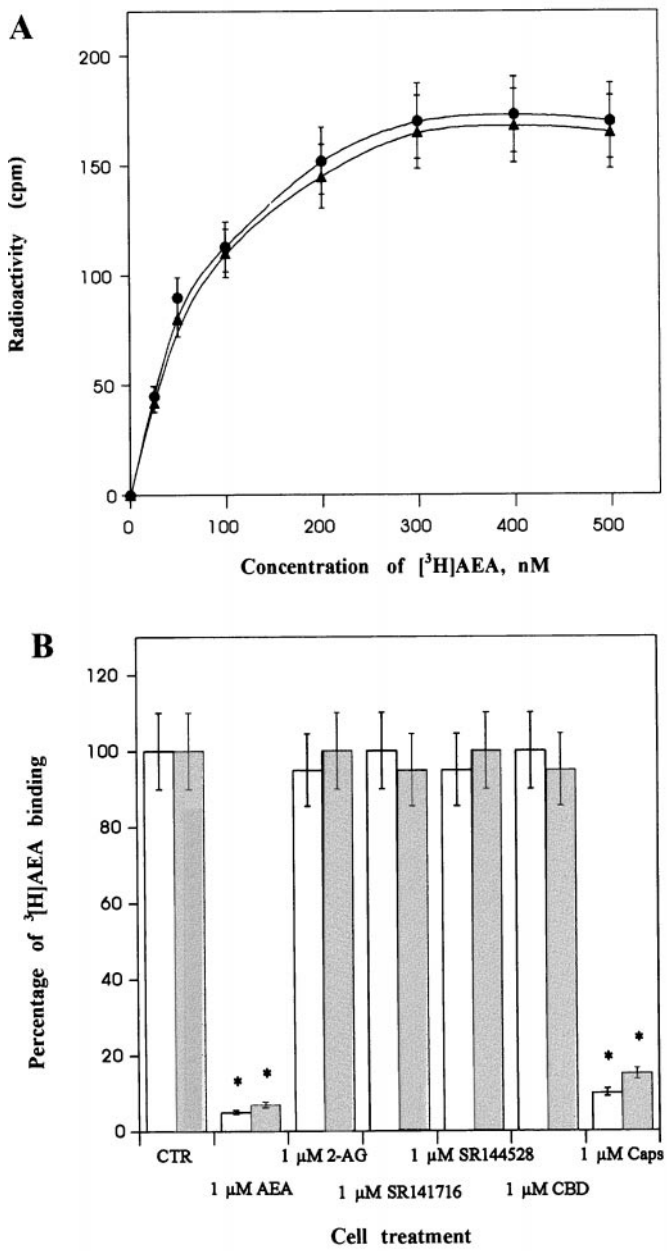

FIG. 3. **Binding of AEA to CHP100 and U937 cells.** *A,* represents the binding of [^{3}H]AEA to CHP100 (*circles*) or U937 (*triangles*) cells. *B*, the effect of (cold) AEA, 2-AG, SR141716, SR144528, CBD, or Caps (each used at 1 μM) on the binding of 200 nM [^{3}H]AEA to CHP100 (*white bars*) or U937 (*gray bars*) is shown, and values were expressed as percentage of the untreated controls (100% = 170 ± 20 (CHP100) or 160 ± 20 (U937) cpm, respectively). *CTR,* control. *, $p < 0.01$ compared with control cells.

pendent mitochondrial uncoupling, which was most evident 6 h after treatment of CHP100 or U937 cells (Table IV). At this time interval, the increase in mitochondrial uncoupling was already significant with 0.25 μM AEA, a concentration that also induced significant apoptotic body formation (Fig. 1). Treatment with AEA also caused a dose-dependent and rapid (within 6 min) increase of intracellular calcium concentration (Table IV). Again, AM404 or ATFMK (both at 10 μM) significantly potentiated, whereas 10 μM Caps inhibited, the effect of AEA on both mitochondrial uncoupling and calcium rise (Table IV). Instead, 2-AG and the other endocannabinoids did not affect mitochondrial integrity or intracellular calcium concentration (Table I). Interestingly, 50 μM EGTA-AM, a permeant calcium chelator (31), reduced the number of apoptotic bodies induced by AEA to approximately 40 or 35% of the control, in CHP100 or U937 cells, respectively (Table II). Also 10 μM ETYA or 10 μM MK886, specific 5-lipoxygenase inhibitors (32, 33), reduced to approximately 40–50% the pro-apoptotic activity of AEA in both cell lines (Table II). Similar results were observed by treating the cells with 10 μM indomethacin, a cyclooxygenase inhibitor (34). Instead, treatment with 10 μM cyclosporin A, a mitochondrial permeability transition pore inhibitor (35), or 50 μM L-NAME, a nitric oxide synthase inhibitor (20), were ineffective (Table II).

Western blot showed that anti-cytochrome *c* monoclonal antibodies specifically recognized a single immunoreactive band in CHP100 and U937 cell saps, corresponding to a molecular mass of approximately 15 kDa (Fig. 4*A*). These antibodies were used to quantify cytochrome *c* release into cell cytosol by ELISA. Treatment of CHP100 or U937 cells with 1 μM AEA led to a 3–3.5-fold increase in cytochrome *c* release after 8 h, an effect that was not prevented by 5 μM SR141716, 5 μM SR144528, or 10 μM CBD (Fig. 4*B*). 10 μM AM404 or 10 μM ATFMK enhanced cytochrome *c* release up to approximately 5-fold over the controls, whereas 10 μM Caps fully inhibited cytochrome *c* release induced by 1 μM AEA in both cell lines (Fig. 4*B*). 2-AG and the other endocannabinoids did not stimulate cytochrome *c* release in CHP100 or U937 cells, when used at 10 μM (Fig. 4*B* and data not shown). Electrotransfer of anti-cytochrome *c* monoclonal antibodies into U937 cells reduced the number of apoptotic bodies induced by 1 μM AEA after 24 h, from 2.8-fold (Fig. 1*B*) to 1.3-fold over the controls, whereas non-immune mouse serum under the same experimental conditions was ineffective. Since the release of cytochrome *c* can trigger an apoptotic caspase cascade (23, 36, 37), we tested the effect of inhibitors of caspase-3 and caspase-9 on AEA-induced PCD. Table II shows that the caspase-3 inhibitor Z-DEVD-FMK or the caspase-9 inhibitor Z-LEHD-FMK, each used at 50 μM, reduced PCD induced by 1 μM AEA in CHP100 or U937 cells to 20–30% of the controls.

DISCUSSION

We have shown that AEA can induce apoptotic body formation and DNA fragmentation, hallmarks of PCD, in human neuronal and immune cells through a pathway involving rise in intracellular calcium, mitochondrial uncoupling, and cytochrome *c* release. Activation of the arachidonate cascade and of the caspase cascade are critical steps in the death program. The pro-apoptotic activity of AEA was observed at physiological concentrations of this compound (24). Unlike AEA, other structurally related and biologically active endocannabinoids, such as 2-AG, LEA, OEA, and PEA (1–3), were unable to force cells into PCD under the same experimental conditions (Table I), ruling out the possibility that the observed effects of AEA were due to unspecific cell poisoning. Since 2-AG may release arachidonate through FAAH activity faster than AEA (38), the lack of pro-apoptotic activity of this compound rules out the possibility that AEA-induced PCD might be due to arachidonate, as reported for U937 cells (39). Consistently, inhibition of FAAH by ATFMK potentiated, instead of reducing, the apoptotic activity of AEA (Table II). Also inhibition of AEA degradation by blocking its uptake enhanced AEA-induced PCD (Table II). Since a slower degradation leads to an increased concentration of AEA in the extracellular matrix, these findings suggest that the pro-apoptotic activity of AEA is mediated by a target molecule on the cell surface. Indeed, [^{3}H]AEA binds to CHP100 and U937 cell membranes (Fig. 3*A*). However, in these cell lines a different binding site must be involved because the "classical" CB1 or CB2 receptors are not present (Fig. 2). Previous reports have shown that AEA can bind and modulate receptors other than CB1R and CB2R (40), and recently a CB receptor for AEA,

TABLE III

Effect of various compounds on AEA-induced cell death in rat C6 and human DAUDI cells

Values in parentheses represent percentage of AEA-treated samples. Treatment of either cell line with any of the compounds listed, in the absence of AEA, did not significantly affect cell death under the same experimental conditions.

Sample	Apoptotic bodies	
	C6	DAUDI
	-fold over control	
Control	1	1
AEA (10 μM)	3.5 ± 0.4 (100)	4.0 ± 0.4 (100)
AEA (10 μM) + SR141716 (1 μM)	6.2 ± 0.6[a] (177)	4.6 ± 0.5[b] (115)
AEA (10 μM) + SR144528 (1 μM)	3.9 ± 0.4[b] (111)	7.2 ± 0.7[a] (180)
AEA (10 μM) + AM404 (10 μM)	6.3 ± 0.6[a] (180)	7.0 ± 0.7[a] (175)
AEA (10 μM) + SR141716 (1 μM) + AM404 (10 μM)	9.5 ± 1.0[a,c] (271)	7.8 ± 0.8[a,d] (195)
AEA (10 μM) + SR144528 (1 μM) + AM404 (10 μM)	7.0 ± 0.7[a,d] (200)	11.4 ± 1.0[a,c] (285)
AEA (10 μM) + CBD (10 μM)	3.7 ± 0.4[b] (106)	4.5 ± 0.5[b] (112)
AEA (10 μM) + Caps (10 μM)	1.5 ± 0.2[a] (43)	1.7 ± 0.2[a] (42)

[a] $p < 0.01$ compared with AEA-treated samples.
[b] $p > 0.05$ compared with AEA-treated samples.
[c] $p < 0.01$ compared with AEA + AM404-treated samples.
[d] $p > 0.05$ compared with AEA + AM404-treated samples.

TABLE IV

Effect of AEA on mitochondrial uncoupling and intracellular calcium concentration in human CHP100 and U937 cells

Values refer to measurements performed 6 h (mitochondrial uncoupling) or 6 min (intracellular calcium) after the addition of each compound.

Compound	Mitochondrial uncoupling		Intacellular calcium	
	CHP100	U937	CHP100	U937
	-fold over control		*-fold over control*	
None	1.0	1.0	1.0	1.0
AM404 (10 μM)	1.0 ± 0.1[a]	1.2 ± 0.1[a]	1.1 ± 0.1[a]	1.0 ± 0.1[a]
ATFMK (10 μM)	1.2 ± 0.1[a]	1.1 ± 0.1[a]	1.0 ± 0.1[a]	1.2 ± 0.1[a]
Caps (10 μM)	1.0 ± 0.1[a]	1.2 ± 0.1[a]	1.1 ± 0.1[a]	1.0 ± 0.1[a]
AEA (0.25 μM)	2.3 ± 0.3[b]	2.4 ± 0.3[b]	2.4 ± 0.3[b]	2.3 ± 0.3[b]
AEA (0.50 μM)	4.5 ± 0.5[b]	4.0 ± 0.4[b]	2.2 ± 0.3[b]	2.4 ± 0.3[b]
AEA (1 μM)	6.3 ± 0.6[b]	5.7 ± 0.6[b]	3.0 ± 0.3[b]	3.2 ± 0.3[b]
AEA (1 μM) + AM404 (10 μM)	10.3 ± 0.9[b,c]	10.9 ± 0.9[b,c]	5.0 ± 0.5[b,c]	5.3 ± 0.5[b,c]
AEA (1 μM) + ATFMK (10 μM)	10.2 ± 0.2[b,c]	10.3 ± 0.2[b,c]	5.2 ± 0.5[b,c]	5.0 ± 0.5[b,c]
AEA (1 μM) + Caps (10 μM)	1.2 ± 0.1[a,d]	1.0 ± 0.1[a,d]	1.1 ± 0.1[a,d]	1.2 ± 0.1[a,d]

[a] $p > 0.05$ compared with control.
[b] $p < 0.01$ compared with control.
[c] $p < 0.05$ compared with AEA (1 μM).
[d] $p < 0.01$ compared with AEA (1 μM).

distinct from type 1 or type 2, has been described in endothelial cells (27). However, this new CB receptor was not expressed in CHP100 or U937 cells, because its selective antagonist CBD (27) was ineffective on [^{3}H]AEA binding (Fig. 3*B*) and on AEA-induced PCD (Table II). On the other hand, it is becoming increasingly evident that AEA behaves as a full agonist at human vanilloid receptors (28, 41), whose activation can induce apoptosis in neuronal (42) and immune (43) cells. Therefore, the possibility that the pro-apoptotic activity of AEA might occur through this receptor was investigated. Indeed, it was found that capsazepine, a selective antagonist of VR (28), prevented [^{3}H]AEA binding to CHP100 or U937 cells (Fig. 3*B*) and inhibited AEA-induced PCD (Table II), whereas the VR agonist capsaicin (28) mimicked the pro-apoptotic activity of AEA in these cells. Altogether, these findings suggest that AEA-induced PCD was mediated by vanilloid receptors. It should be stressed that this hypothesis is consistent with the observation that 2-AG and the other endocannabinoids did not promote PCD (Table I), because these compounds do not activate vanilloid receptors (28) or have a much lower potency than AEA (44). In this context, it seems noteworthy that AM404 alone was ineffective on PCD, mitochondrial uncoupling, intracellular calcium concentration, or cytochrome *c* release from cells, although it did potentiate the effect of AEA (Tables II–IV and Fig. 4*B*). These findings suggest that AM404 was unable to activate directly human VR, at variance with a previous report suggesting that it is an agonist for rat VR (41).

A major finding of this investigation is that CB1R or CB2R antagonists, SR141716 or SR144528, were ineffective in CHP100 or U937 cells, which lack cannabinoid receptors (Fig. 2), but they did potentiate AEA-induced PCD in C6 or DAUDI cells (Table III). In fact, these cells express functional CB1 or CB2 receptors, respectively (Fig. 2), and were able to bind larger amounts of [^{3}H]AEA than CHP100 or U937 cells. Capsazepine displaced approximately 30% [^{3}H]AEA from C6 or DAUDI cells, suggesting that the remaining 70% was bound to CB receptors. Remarkably, capsazepine prevented AEA-induced PCD in these cells in a way fully analogous to that observed in CHP100 or U937 cells (Table III), suggesting that vanilloid receptors mediate the pro-apoptotic activity of AEA also in C6 and DAUDI cells. As a matter of fact, specific vanilloid responses have been described in C6 cells (45). Like in CHP100 or U937 cells, cannabidiol was ineffective on the pro-apoptotic activity of AEA in C6 or DAUDI cells, ruling out that

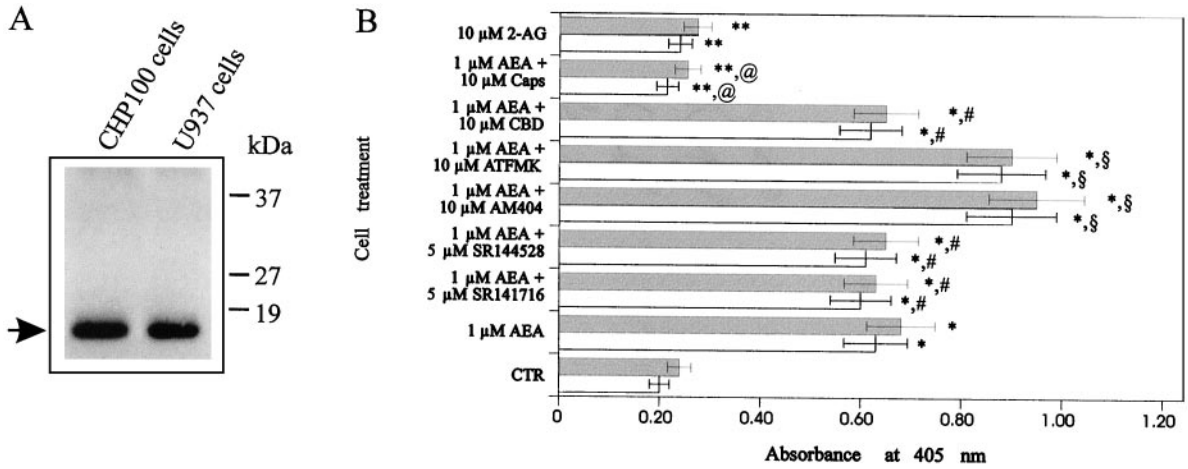

FIG. 4. **Effect of AEA on cytochrome *c* release from CHP100 and U937 cells.** *A* shows Western blot analysis of cytochrome *c* in cell homogenates (25 μg/lane). The *arrow* indicates the expected molecular size for cytochrome *c*. Molecular mass markers are shown on the *right-hand side*. *B* shows the effect of 1 μM AEA, in the absence or in the presence of 5 μM SR141716, 5 μM SR144528, 10 μM AM404, 10 μM ATFMK, 10 μM CBD, or 10 μM Caps, on cytochrome *c* release from CHP100 (*white bars*) or U937 (*gray bars*) cells, as determined by ELISA at 405 nm (see "Experimental Procedures"). Treatment of either cell line with any of the compounds listed, in the absence of AEA, was ineffective under the same experimental conditions. *CTR,* control. *, $p < 0.01$ compared with control cells; **, $p > 0.05$ compared with control cells; #, $p > 0.05$ compared with AEA-treated cells; §, $p < 0.05$ compared with AEA-treated cells; @, $p < 0.01$ compared with AEA-treated cells.

the new "endothelial" CBR (27) might be involved. On the other hand, it seems noteworthy that the ability of C6 or DAUDI cells to degrade AEA through intracellular uptake and degradation by FAAH was similar to that of CHP100 or U937 cells, respectively. Therefore, it is tempting to speculate that cells bearing functional CB1 or CB2 receptors on their surface are protected against the toxic effects of physiological concentrations of AEA. In C6 or DAUDI cells, the effects on PCD of co-administration of the transporter inhibitor AM404, which increases extracellular concentration of AEA, or of CBR antagonists SR141716 and SR144528, which prevent CBR activation (Table III), support this concept. These findings can be interpreted by suggesting a regulatory loop between CB receptors and the AEA transporter, which has been recently demonstrated in human endothelial cells (13). In this loop, the binding of AEA to CB receptors triggers the activation of AEA uptake by cells, followed by intracellular degradation of AEA by FAAH. Elimination of AEA from the extracellular space might terminate its activity at vanilloid receptors, thus inhibiting the induction of apoptosis. Scheme I summarizes the main features of this model.

PCD of CHP100 or U937 cells induced by AEA was executed through a series of events common to several types of unrelated apoptotic stimuli (46). It involved the following: (i) rise in cytosolic calcium concentration (within 6 min), (ii) uncoupling of mitochondria (within 6 h), and (iii) release of cytochrome *c* (within 8 h). These events required gene expression of proteins necessary for apoptosis, as shown by the protective effect of actinomycin D and cycloheximide (Table II). Consistently with the data on apoptotic body formation and [^{3}H]AEA binding to cell membranes, (i) capsazepine inhibited the events triggered by AEA, (ii) AM404 or ATFMK potentiated them, and (iii) SR141716, SR144528, or CBD were ineffective (Table IV and Fig. 4*B*). At variance with other types of PCD (47), calcium rise induced by AEA was not acting through activation of nitric-oxide synthase, because the nitric-oxide synthase inhibitor L-NAME was ineffective in protecting cells against AEA. Instead, arachidonate degradation by 5-lipoxygenase and cyclooxygenase activities, which might be enhanced as a consequence of a rise in intracellular Ca^{2+} (32–34), had a role in the process, because the inhibitors ETYA and MK886 significantly inhibited AEA-induced PCD (Table II). It must be mentioned that MK886 can exert lipoxygenase-unrelated effects on mammalian cells (33). However, the observation that ETYA and MK886 yielded the same inhibition of apoptosis seems to rule out the involvement of lipoxygenase-independent pathways. This seems interesting, because formation of arachidonate products unbalances the intracellular redox level and has been implicated in apoptotic death of several cell types (7, 17, 33, 39). In particular, it should be stressed that a function for lipoxygenase in programmed organelle degradation has been recently demonstrated, showing that the enzyme can make pore-like structures in the lipid bilayer (48). This activity might contribute to uncouple directly the mitochondria (Table IV). However, opening of the mitochondrial permeability transition pore (35)

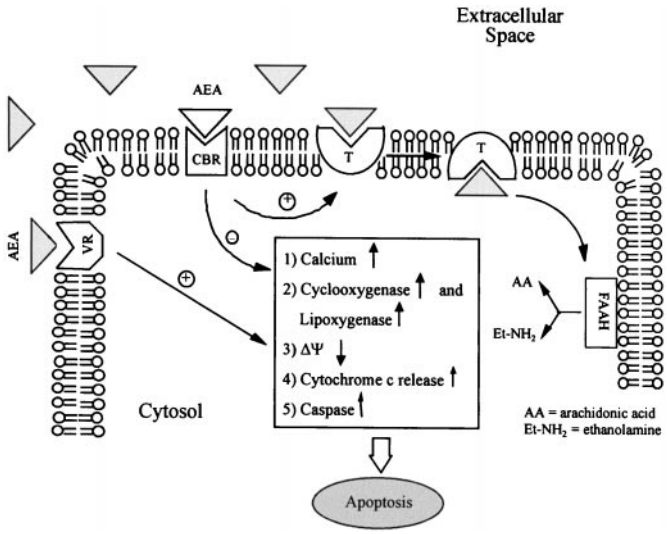

SCHEME I. **Role of vanilloid receptor and cannabinoid receptor in AEA-induced programmed cell death**. Binding of extracellular AEA to VR triggers a sequence of events starting with a rise in intracellular calcium and followed by activation of cyclooxygenase and lipoxygenase, drop in mitochondrial membrane potential ($\Delta\psi$), release of cytochrome *c,* and activation of caspases, ultimately leading to programmed cell death (apoptosis). Binding of AEA to cannabinoid receptors (*CBR*) activates transporter (*T*)-mediated uptake of AEA and its subsequent cleavage to arachidonic acid and ethanolamine by membrane-bound FAAH. These latter events inhibit the pro-apoptotic activity of AEA.

did not contribute to AEA-induced PCD, as suggested by the lack of effect of cyclosporin A (Table II). On the other hand, an unbalanced redox level in the cell has been associated to release of cytochrome *c*, a converging point in apoptosis induced by different stimuli in various cell types (23, 36, 46, 47). Cytochrome *c* release was observed also in AEA-induced PCD (Fig. 4*B*), and it was essential for apoptosis, because sequestering cytochrome *c* within intact U937 cells by electrotransferred anti-cytochrome *c* monoclonal antibodies was able to prevent AEA-induced PCD (37). Cytochrome *c* release in the cell cytosol is usually followed by activation of a caspase cascade, initiated by caspase-3 and caspase-9 which are the most proximal members of the proteolytic chain (23, 36, 37). Caspases are thought to form a proteolytic machinery within the cell, resulting in the breakdown of key enzymes and cellular structures, and to activate DNases responsible for chromatin degradation seen in apoptosis (37). Also AEA-induced PCD seemed to be executed through this series of events, because caspase-3 or caspase-9 inhibitors reduced apoptotic body formation to approximately 20–30% of the controls (Table II). Altogether, these results suggest that PCD induced by AEA occurs through an apoptotic pathway based on calcium rise, mitochondrial uncoupling, and cytochrome *c* release. Upstream activation of the arachidonate cascade leads to redox unbalance and organelle disruption, which both favor cytochrome *c* release, then caspases act as downstream executioners of the death program. In this context, it seems noteworthy that also capsaicin-induced PCD occurs through intracellular calcium rise, imbalance of the redox level, and drop in mitochondrial membrane potential (43), further strengthening the hypothesis that AEA is acting through vanilloid receptors. Scheme I summarizes the series of events responsible for AEA-induced cell death. It seems noteworthy that these findings might be relevant also for neuronal apoptosis induced by alcohols (49), where an increase in AEA concentration has been reported (50). Moreover, they demonstrate major differences in the cytotoxicity of the different endocannabinoids, which might be relevant for understanding their pathophysiological roles (1–3). Finally, this study shows that endocannabinoids exert similar actions in neuronal and immune cells, perhaps (and significantly) through common signals.

Acknowledgments—We thank Dr. Dale G. Deutsch (Department of Biochemistry and Cell Biology, State University of New York, Stony Brook) for the kind gift of C6 glioma cells, Drs. Marco Ranalli and Rita Agostinetto for their skillful assistance with cytofluorimetric analysis and cell culture, and Dr. Francesca Bernassola for helpful discussions.

REFERENCES

1. Pop, E. (1999) *Curr. Opin. Chem. Biol.* **3,** 418–425
2. Di Marzo, V., Bisogno, T., De Petrocellis, L., Melck, D., Orlando, P., Wagner, J. A., and Kunos, G. (1999) *Eur. J. Biochem.* **264,** 258–267
3. Pertwee, R. G. (1997) *Pharmacol. Ther.* **74,** 129–180
4. De Petrocellis, L., Melck, D., Palmisano, A., Bisogno, T., Laezza, C., Bifulco, M., and Di Marzo, V. (1998) *Proc. Natl. Acad. Sci. U. S. A.* **95,** 8375–8380
5. Derocq, J.-M., Bouaboula, M., Marchand, J., Rinaldi-Carmona, M., Ségui, M., and Casellas, P. (1998) *FEBS Lett.* **425,** 419–425
6. Schwarz, H., Blanco, F. J., and Lotz, M. (1994) *J. Neuroimmunol.* **55,** 107–115
7. Sarker, K. P., Obara, S., Nakata, M., Kitajima, I., and Maruyama, I. (2000) *FEBS Lett.* **472,** 39–44
8. Galve-Roperh, I., Sànchez, C., Cortes, M. L., del Pulgar, T. G., Izquierdo, M., and Guzman, M. (2000) *Nat. Med.* **6,** 313–316
9. Sànchez, C., Galve-Roperh, I., Canova, C., Brachet, P., and Guzmàn, M. (1998) *FEBS Lett.* **436,** 6–10
10. Chan, G. C.-K., Hinds, T. R., Impey, S., and Storm, D. R. (1998) *J. Neurosci.* **18,** 5322–5332
11. Ruiz, L., Miguel, A., and Diaz-Laviada, I. (1999) *FEBS Lett.* **458,** 400–404
12. Walker, J. M., Huang, S. M., Strangman, N. M., Tsou, K., and Sañudo-Peña, M. C. (1999) *Proc. Natl. Acad. Sci. U. S. A.* **96,** 12198–12203
13. Maccarrone, M., Bari, M., Lorenzon, T., Bisogno, T., Di Marzo, V., and Finazzi-Agrò, A. (2000) *J. Biol. Chem.* **275,** 13484–13492
14. Maccarrone, M., Valensise, H., Bari, M., Lazzarin, N., Romanini, C., and Finazzi-Agrò, A. (2000) *Lancet* **355,** 1326–1329
15. Maccarrone, M., van der Stelt, M., Rossi, A., Veldink, G. A., Vliegenthart, J. F. G., and Finazzi-Agrò, A. (1998) *J. Biol. Chem.* **273,** 32332–32339
16. Maccarrone, M., Veldink, G. A., and Vliegenthart, J. F. G. (1992) *Eur. J. Biochem.* **205,** 995–1001
17. Maccarrone, M., Catani, M. V., Finazzi-Agrò, A., and Melino, G. (1997) *Cell Death Differ.* **4,** 396–402
18. Maccarrone, M., Nieuwenhuizen, W. F., Dullens, H. F. J., Catani, M. V., Melino, G., Veldink, G. A., Vliegenthart, J. F. G., and Finazzi-Agrò, A. (1996) *Eur. J. Biochem.* **241,** 297–302
19. Maccarrone, M., Fiorucci, L., Erba, F., Bari, M., Finazzi-Agrò, A., and Ascoli, F. (2000) *FEBS Lett.* **468,** 176–180
20. Deutsch, D. G., Goligorsky, M. S., Schmid, P. C., Krebsbach, R. J., Schmid, H. H. O., Das, S. K., Dey, S. K., Arreaza, G., Thorup, C., Stefano, G., and Moore, L. C. (1997) *J. Clin. Invest.* **100,** 1538–1546
21. Smiley, S. T. (1991) *Proc. Natl. Acad. Sci. U. S. A.* **88,** 3671–3675
22. Vandenberghe, P. A., and Ceuppens, J. L. (1990) *J. Immunol. Methods* **127,** 197–205
23. Ushmorov, A., Ratter, F., Lehmann, V., Dröge, W., Schirrmacher, V., and Umansky, V. (1999) *Blood* **93,** 2342–2352
24. Di Marzo, V., Sepe, N., De Petrocellis, L., Berger, A., Crozier, G., Fride, E., and Mechoulam, R. (1998) *Nature* **396,** 636
25. Piomelli, D., Beltramo, M., Glasnapp, S., Lin, S. Y., Goutopoulos, A., Xie, X. Q., and Makriyannis, A. (1999) *Proc. Natl. Acad. Sci. U. S. A.* **96,** 5802–5807
26. Koutek, B., Prestwich, G. D., Howlett, A. C., Chin, S. A., Salehani, D., Akhavan, N., and Deutsch, D. G. (1994) *J. Biol. Chem.* **269,** 22937–22940
27. Járai, Z., Wagner, J., Varga, K., Lake, K. D., Compton, D. R., Martin, B. R., Zimmer, A. M., Bonner, T. I., Buckley, N. E., Mezey, E., Razdan, R. K., Zimmer, A., and Kunos, G. (1999) *Proc. Natl. Acad. Sci. U. S. A.* **96,** 14136–14141
28. Zygmunt, P. M., Petersson, J., Andersson, D. A., Chuang, H.-H., Sorgård, M., Di Marzo, V., Julius, D., and Högestätt, E. D. (1999) *Nature* **400,** 452–457
29. Deutsch, D. G., and Chin, S. A. (1993) *Biochem. Pharmacol.* **46,** 791–796
30. Galiègue, S., Mary, S., Marchand, J., Dussossoy, D., Carrière, D., Carayon, P., Bouaboula, M., Shire, D., Le Fur, G., and Casellas, P. (1995) *Eur. J. Biochem.* **232,** 54–61
31. Maki, A., Berezesky, I. K., Fargnoli, J., Holbrook, N. J., and Trump, B. F. (1992) *FASEB J.* **6,** 919–924
32. Ford-Hutchinson, A. W., Gresser, M., and Young, R. N. (1994) *Annu. Rev. Biochem.* **63,** 383–417
33. Datta, K., Biswal, S. S., Xu, J., Towndrow, K. M., Feng, X., and Kehrer, J. P. (1998) *J. Biol. Chem.* **273,** 28163–28169
34. Ara, G., and Teicher, B. A. (1996) *Prostaglandins Leukot. Essent. Fatty Acids* **54,** 3–16
35. Andreyev, A., and Fiskum, G. (1999) *Cell Death Differ.* **6,** 825–832
36. Garrido, C., Bruey, J.-M., Fromentin, A., Hammann, A., Arrigo, A. P., and Solary, E. (1999) *FASEB J.* **13,** 2061–2070
37. Neame, S. J., Rubin, L. L., and Philpott, K. L. (1998) *J. Cell Biol.* **142,** 1583–1593
38. Goparaju, S. K., Ueda, N., Yamaguchi, H., and Yamamoto, S. (1998) *FEBS Lett.* **422,** 69–73
39. Vanags, D. M., Larsson, P., Feltenmark, S., Jakobsson, P.-J., Orrenius, S., Claesson, H.-E., and Aguilar-Santelises, M. (1997) *Cell Death Differ.* **4,** 479–486
40. Wagner, J. A., Varga, C., Jàrai, Z., and Kunos, G. (1999) *Hypertension* **33,** 429–434
41. Smart, D., and Jerman, J. C. (2000) *Trends Pharmacol. Sci.* **21,** 134
42. Sugimoto, T., Takeyama, A., Xiao, C., Takano-Yamamoto, T., and Ichikawa, H. (1999) *Brain Res.* **818,** 147–152
43. Macho, A., Calzado, M. A., Munoz-Blanco, J., Gomez-Diaz, C., Gajate, C., Mollinedo, F., Navas, P., and Munoz, E. (1999) *Cell Death Differ.* **6,** 155–165
44. Smart, D., Gunthorpe, M. J., Jerman, J. C., Nasir, S., Gray, J., Muir, A. I., Chambers, J. K., Randall, A. D., and Davis, J. B. (2000) *Br. J. Pharmacol.* **129,** 227–230
45. Bíró, T., Brodie, C., Modarres, S., Lewin, N. E., Ács, P., and Blumberg, P. M. (1998) *Mol. Brain Res.* **56,** 89–98
46. Wallace, D. C. (1999) *Science* **283,** 1482–1493
47. Ghafourifar, P., Klein, S. D., Schucht, O., Schenk, U., Pruschy, M., Rocha, S., and Richter, C. (1999) *J. Biol. Chem.* **274,** 6080–6084
48. Van Leyen, K., Duvoisin, R. M., Engelhardt, H., and Wiedmann, M. (1998) *Nature* **395,** 392–395
49. Saito, M., Saito, M., Berg, M. J., Guidotti, A., and Marks, N. (1999) *Neurochem. Res.* **24,** 1107–1115
50. Basavarajappa, B. S., and Hungund, B. L. (1999) *J. Neurochem.* **72,** 522–528